

## B. PHYSICS OF TRAPPED IONS

The study of nuclei stored in traps grows in importance for our group. Our theoretical investigation of the dynamics of trapped ions continue. The Canadian Penning Trap (CPT) has now become a rich source of new measurements, both for astrophysics and for weak interaction physics. The Advanced Penning Trap (APT) is under construction, with a goal to studying weak interactions in calendar year 2005. The laser atom trap (ATTA) is online and made its first measurements on radioactive  ${}^6\text{He}$  and investigation of a possible measurement of  ${}^8\text{He}$  is underway.

### b.1. Ordering and Temperature in Ions Trapped in Radiofrequency Fields (J. P. Schiffer)

Some time ago simulations were carried out to better understand the behavior of plasmas confined in radiofrequency traps.<sup>1</sup> In that study it was found that if a plasma was cooled to an ordered state, the kinetic energy in the rf motion, which can be 5-6 orders of magnitude more than the energy corresponding to the temperature, converted into random thermal energy only very slowly – in less than  $\sim 10^{12}$  rf periods for a sufficiently cold system.

However, when the ion cloud in the simulation was warmer, this conversion (the coupling of the periodic motion from the confining field into random motion) occurred faster, and this "rf heating" increased quadratically with temperature. The reason for such a  $T^2$  dependence is not understood.

Radiofrequency traps can work with a variety of rf wave forms. In the work of Ref. 1 it was assumed to be sinusoidal. In order to explore whether the

behavior was similar for other wave forms a simulation is carried out where the rf containing field is a square wave rather  $\sin(\omega t)$ . A cold ordered state was achieved in this system and, as was reported last year, the self-heating (the above coupling of the periodic motion into thermal energy) appears to be much smaller.

The phenomenon has been explored more carefully in the past year. The simulations are extremely time consuming. The very surprising result is that the systems considered (square-wave rf confinement, or "pulsed" rf fields that are applied periodically in opposite directions) the isolated confined systems instead of "self heating" actually seem to be getting slowly "colder" in time as is shown in Fig. I-7. Since the forced oscillations imposed by the confining field provide a large reservoir of energy, no conservation laws or thermodynamic principles are obviously violated. Yet the phenomenon is completely unexpected and counter-intuitive. It is being explored more thoroughly.

<sup>1</sup>J. P. Schiffer *et al.*, Proc. Natl. Acad. Sci. **10**, 1073 (2000).

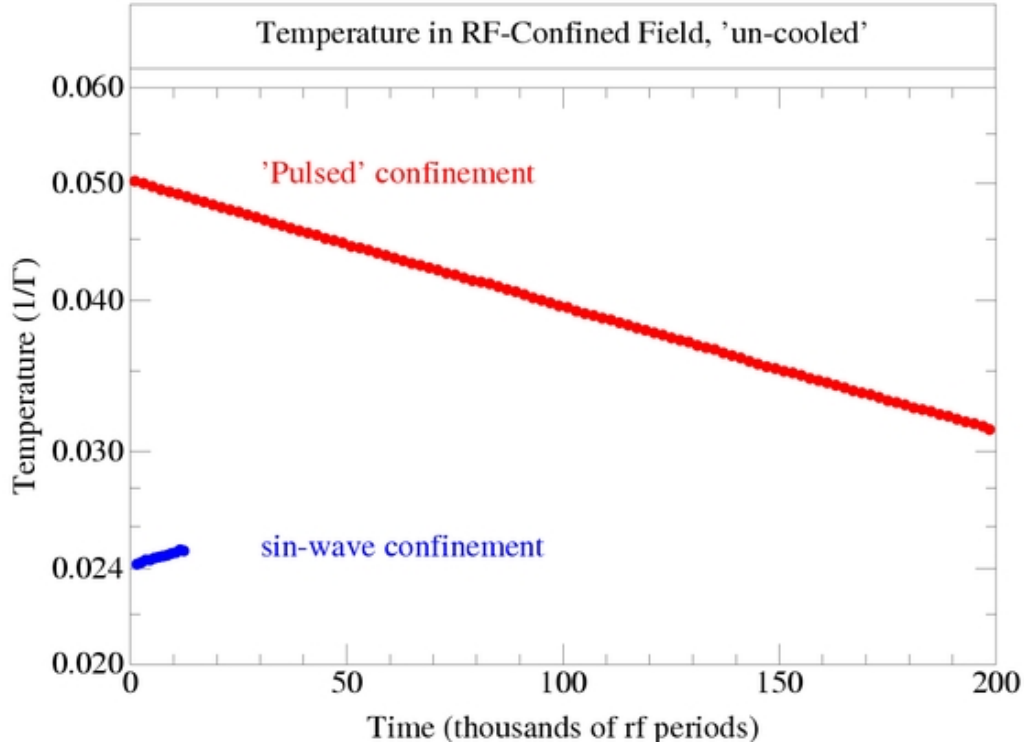


Fig. I-7. The "temperature" (derived from the velocities that are not periodic in the imposed rf confining field) is plotted from the simulation of a confined system of 1000 particles. The simulated confinement is that characteristic of rf quadrupole traps. Temperature is in units of  $1/\Gamma$ , where  $\Gamma = (q^2/a)/kT$ , the plasma coupling parameter. The normal transition temperature to an ordered system is  $1/\Gamma \approx 0.006$ . The blue points represent the behavior of 1000 ions that are confined in a sinusoidally periodic field and allowed to interact with each other through their Coulomb interactions. They show the usual "rf heating" effect. The red points are from a long simulation where the confining field is "pulsed": periodic short pulses of electric field alternating in sign. This system appears to have a gradually lower "temperature".

**b.2. Q Value of the Superallowed  $\beta$ -Decay of  $^{22}\text{Mg}$  and the Calibration of the  $^{21}\text{Na}(p,\gamma)$  Reaction** (G. Savard,\* J. A. Clark,† A. A. Hecht,‡ A. F. Levand, B. F. Lundgren, N. D. Scielzo, I. Tanihata, W. Trimble, J. C. Wang,† Z. Zhou, F. Buchinger,§ J. E. Crawford,§ S. Gulick,§ J. C. Hardy,¶ V. E. Iacob,¶ J. K. P. Lee,§ K. S. Sharma,|| I. S. Towner,\*\* and Y. Wang||)

Superallowed  $0^+ \rightarrow 0^+$  decays play a key role in a number of tests of the electroweak theory. The  $Ft$  value for such decays, obtained from measurements of the lifetime,  $Q$  value and branching ratio, can be corrected for small radiative and isospin mixing effects to yield a corrected  $Ft$  value, which has the simple form

$$Ft \equiv ft(1 + \delta_R')(1 + \delta_{NS} - \delta_C) = \frac{K}{2G_V^2(1 + \Delta_R^V)},$$

with  $f$  being the statistical rate function,  $t$  the partial half-life,  $G_V$  the weak vector coupling constant, and  $K$  is a numerical constant. The small correction

terms include  $\delta_C$ , the isospin symmetry-breaking correction,  $\delta_R'$  and  $\delta_{NS}$ , the transition-dependent parts of the radiative correction, and  $\Delta_R^V$  the transition-independent part. Only  $\delta_C$  and  $\delta_{NS}$  depend on nuclear structure.

The Conserved Vector Current (CVC) hypothesis states that the vector current interaction is not modified by the presence of the strongly interacting nuclear system so that exactly the same value of  $G_V$  should be obtained from each superallowed decay. The existing set of nine precisely determined transitions confirms this CVC expectation at the  $3 \times 10^{-4}$  level. The resultant average

value of  $G_V$ , together with the Fermi coupling constant from the pure-leptonic decay of the muon, yields the most precise available value for  $V_{ud}$ , the up-down quark mixing element of the Cabibbo-Kobayashi-Maskawa (CKM) matrix. This matrix is a rotation matrix connecting the weak and mass eigenstates of the quarks and, as such, must be unitary within the standard model. Currently, the most demanding test of CKM unitarity comes from the top-row sum,

$$V_{ud}^2 + V_{us}^2 + V_{ub}^2 = 0.9968 \pm 0.0014,$$

which actually violates unitarity at the 2.3 sigma level. The main contributors to that unitarity test are  $V_{ud}$  and  $V_{us}$ , which contribute almost equally to the total uncertainty. This discrepancy has attracted considerable attention and both  $V_{ud}$  and  $V_{us}$  are now under much scrutiny. Recent work indicates that the value of  $V_{us}$  might have to be shifted to one yielding a better agreement with unitarity; if this is confirmed it would only further fuel the need for a more precise  $V_{ud}$  value.

We report here a  $Q$ -value measurement for the  $^{22}\text{Mg}$  decay, which complements recent lifetime and branching-ratio measurements<sup>1</sup> to yield a precise  $Ft$  value for its superallowed transition. This is the first new superallowed case in a region of well-understood nuclear structure and consequently is the first significant step in testing the validity of the calculated structure-dependent corrections.

The mass measurements were performed at the Canadian Penning Trap (CPT) mass spectrometer located "online" at the ATLAS accelerator. The  $^{22}\text{Mg}$  and  $^{22}\text{Na}$  activities were created by a 3.5 MeV/u beam of  $^{20}\text{Ne}$  passing through a 7 cm long cryogenic target of  $^3\text{He}$  gas held at a pressure of 700 mbar and liquid nitrogen temperature. The gas target has 1.3 mg/cm<sup>2</sup> thick titanium entrance and exit windows. Reaction products recoiling out of the target are carried forward by the kinematics of the reaction. They then proceed through a focusing magnetic quadrupole triplet, a velocity filter to separate the primary beam from the reaction products, and an Enge magnetic spectrograph to make the final selection and focus them on the entrance of a gas catcher system. At that point, the species of interest forms a multi-MeV continuous beam of poor ion-optical quality quite unsuitable for efficient injection into a precision ion trap, which requires a high quality eV-energy pulsed beam. We

achieve the required transformation of beam properties with a gas catcher and injection system.

At the entrance of the gas catcher system, the reaction products lose most of their energy through a thin aluminum foil that can be rotated to adjust the effective thickness and hence the energy lost by the ions. The tunable aluminum degrader is followed by a high-purity 25 cm long helium gas cell. The radioactive ions enter this gas cell through a 1.9 mg/cm<sup>2</sup> Havar window, losing their remaining energy and then coming to rest in the helium gas, which is pure to the ppb level and is held at roughly 150 mbar pressure. At the final stage of their slowing-down process, the ions, which have been highly charged up to this point, recapture electrons but are unlikely to recapture the final electron since helium has a higher ionization potential than any other species and hence will not give up its electrons to slow ions. The radioactive species are therefore stopped as ions in the high-purity gas and can be manipulated by static and RF electric fields. With the assistance of these electric fields, the ions are extracted from the gas cell in roughly 10 ms as a thermal beam. The ions are then separated from the helium gas extracted with them by being channeled through RF ion guides leading to a linear RF trap, where they are accumulated. The ions in the linear trap are accumulated for 300 ms and transferred in a bunch to a gas-filled Penning trap where mass-selective cooling is applied. The ions are mass selected there with a resolution of 1000 before being transported to the CPT spectrometer itself.

Also present after the gas cell are ions of helium and impurities ionized in the deceleration of the radioactive ions in the helium gas. The helium ions are easily eliminated by the RF ion guide system, but it was found that by focusing on  $A = 22$  this experiment incurred a particular difficulty since neon is a common impurity in even the highest purity helium gas. We found that we could not discriminate against the  $^{22}\text{Ne}$  isotope, so this isotope saturated the system. The difficulty was overcome by the addition of a cold trap, temperature-regulated at 20 - 30 K, in the helium purification system to remove the neon from the helium gas being fed into the gas cell. With this modification, the mass-22 radioactive ions were collected free of other contamination. The purified radioactive ions with  $A = 22$  were transported in bunched mode to the CPT, where the ions were captured in a second linear RF trap and further cooled by buffer-gas collisions before being transferred via a differential pumping section to the precision Penning trap, where the mass measurements take place.

The precision Penning trap is a hyperbolic trap with gold-plated OFHC copper electrodes located in a 6T self-shielded superconducting magnet with high field stability. The trap is in  $10^{-10}$  mbar vacuum section and all material used inside the magnet is non-magnetic, including the vacuum chamber, which is made of molybdenum. This not only avoids perturbations in the homogeneity of the magnetic field but also removes a common source of magnetic-field fluctuations connected to the temperature-dependent magnetic properties of the "non-magnetic" stainless-steel vacuum chamber typically used. In the Penning trap, a mass measurement is performed as a frequency scan. The ions are first loaded into the trap. Remaining contaminant ions (in this case, either mostly  $^{22}\text{Na}$  when  $^{22}\text{Mg}$  is being measured or the reverse) are removed from the trap by a strong mass-selective RF excitation. The ions of interest are then excited to a finite magnetron orbit by a fixed-frequency dipole RF excitation and are subjected to a quadrupolar RF field, which couples the magnetron and reduced cyclotron motion when the frequency applied corresponds to the true cyclotron frequency. The ions are subsequently ejected and allowed to drift towards a microchannel-plate detector, where a time-of-flight spectrum is recorded. The process is repeated with the injection of another bunch of ions into the trap, repetition of the ion cleaning and preparation, and quadrupolar excitation at the next frequency. This process is continued over the full cyclotron excitation-frequency interval to create a scan, and scans are repeated and summed until sufficient statistics are achieved. At the true cyclotron frequency, the ions will have their magnetron motion converted to reduced cyclotron motion and hence will have higher energy, leading to a reduced time-of-flight to the detector. For these measurements, the excitation time was 0.8 seconds, which yields a mass resolution of  $\sim 2.5 \times 10^{-7}$ .

Our experiment interleaved measurements of the mass of  $^{22}\text{Na}^+$  and  $^{22}\text{Mg}^+$  with calibrations of the magnetic field based on molecular ions of  $\text{H}_2^{18}\text{OH}^+$  and  $\text{H}_2^{16}\text{OH}^+$  and ions of  $^{22}\text{Ne}^+$ ,  $^{21}\text{Ne}^+$  and  $^{20}\text{Ne}^+$ . (Measurements with neon isotopes required our bypassing the 20 K cold trap in the gas purification system.) The results from these calibration

measurements, which were continued over a full week to confirm the stability of the magnetic field, are shown in Fig. I-8. The important features in this figure are the precision, high reproducibility and high stability of the measured masses, which show negligible drift within statistical accuracy over the measurement period. (No correction for field drift is applied in this figure.) The magnetic-field variation was measured to be -1.1 part in  $10^{10}$  per hour. This shift is small at the level of accuracy required since calibration and measurements on radioactive species were interleaved in our case, but all measurements were still corrected for it.

The most insidious source of systematic errors for high-precision measurements on short-lived isotopes in a Penning trap is the possibility that the ions do not probe the same magnetic-field region. No cooling is applied in the measurement trap because of the short time available, and the spatial extent probed by the ions in the trap is determined by the ion preparation and the conditions of injection. The main factor is the timing of the capture pulse applied to let the ions into the measurement trap, which is set by the time-of-flight between the second linear trap, where the cooling is applied, and the measurement trap. For an electrostatic transfer system this time scales as the squared-root of the mass of the transferred ion, but fixed delays in the application of pulses can create small deviations from this simple scaling relation. The capture timing of all measured masses in this experiment was measured precisely and adjusted for the maximum time-of-flight signal of each species. The effectiveness of this procedure is demonstrated in Fig. I-8, which shows that the masses of  $^{20}\text{Ne}$ ,  $^{21}\text{Ne}$ ,  $^{22}\text{Ne}$  and  $\text{H}_2^{16}\text{OH}$ , all known to better than 2 parts per billion, agree within the accuracy of the measurement, which is typically 1 part in  $10^8$ . Although the data show that the use of any of these well known isotopes is equivalent within the statistical accuracy, we have opted to be more conservative and have determined all new masses with respect to a well-known mass with the same A value --  $^{22}\text{Ne}$  for the radioactive ions at A = 22 and  $^{21}\text{Ne}$  for the  $\text{H}_2^{18}\text{OH}$  molecule -- to eliminate any unforeseen mass-dependent effect. We use the 1 part per  $10^8$  accuracy demonstrated in the calibration (on mass ratios involving different mass number) as a conservative value for our systematic error for the new mass values obtained below on ratios of same mass number isotopes.

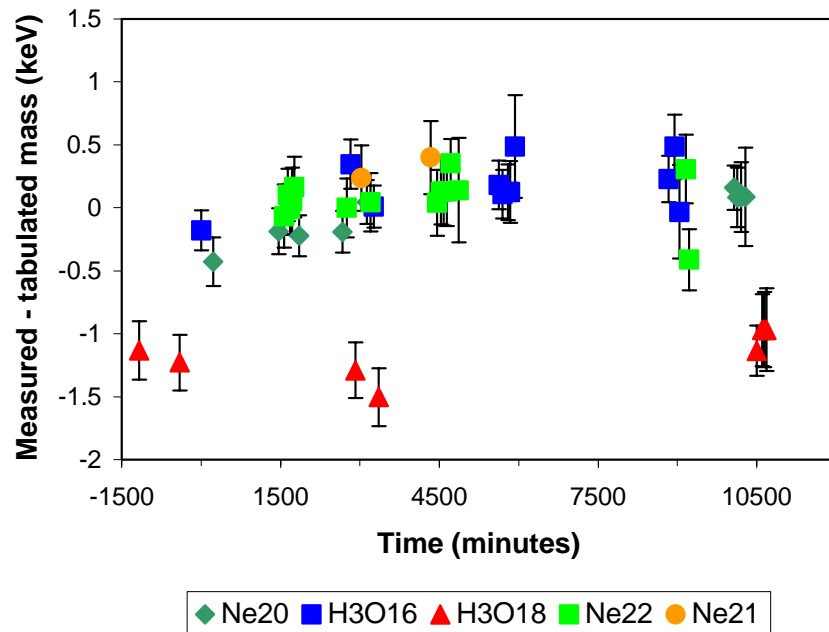


Fig. I-8. Measured mass values (plotted as deviation from the tabulated mass values) for the various isotopes versus time during the run.

Measurements on the stable isotopes and molecules were performed with an average of 1.5 ions detected per cycle; the measurements on  $^{22}\text{Mg}$  and  $^{22}\text{Na}$  had an average of 0.35 and 0.7 ions per cycle, respectively. Shifts in cyclotron frequency due to ion-ion interactions at these low ion numbers were measured to be 2 ppb per detected ion at the CPT. Corrections to account for the lower ion number obtained with the radioactive species compared with that for the stable calibration isotopes are very small but still adjustments of  $0.05 \text{ keV}/c^2$  and  $0.04 \text{ keV}/c^2$  were applied to  $^{22}\text{Mg}$  and  $^{22}\text{Na}$  respectively. Since all measurements on the stable isotopes are made with similar small ion numbers, no adjustments were required among them.

The mass of one of the calibrant molecular ions,  $\text{H}_2^{18}\text{OH}^+$ , is not known to very high accuracy; the uncertainty in its mass is dominated by the  $0.6 \text{ keV}/c^2$  uncertainty in the mass of  $^{18}\text{O}$ . We obtained a mass ratio for  $\text{H}_2^{18}\text{OH}^+$  versus  $^{21}\text{Ne}^+$  of 1.0013712843(65). The  $^{18}\text{O}$  mass determined from this value is found to differ by  $-1.5 \text{ keV}/c^2$  from the tabulated value and yields, after a minute  $-0.02 \text{ keV}$  correction for molecular binding and electronic ionization energy differences, an improved mass defect for  $^{18}\text{O}$  of  $-783.06(23) \text{ keV}$ , with the quoted error containing the statistical and systematic uncertainties added in

quadrature. This measurement of  $^{18}\text{O}$ , via the molecule  $\text{H}_2^{18}\text{OH}$  at mass-21, is consistent with the precisely known calibrations at mass-19, 20, 21 and 22. The previous measurements that have large influence on the tabulated mass<sup>2</sup> of  $^{18}\text{O}$  are inconsistent and are all less precise than the present measurement. Our measurement is compatible with the  $^{18}\text{O}(^3\text{He,p})^{20}\text{F}$  reaction result but disagrees with the mass derived from beta endpoint results.

For the  $A = 22$  radioactive species, the calibration used was  $^{22}\text{Ne}^+$  and the mass ratios observed were 1.000372238(31) and 1.000138820(11) for  $^{22}\text{Mg}^+$  versus  $^{22}\text{Ne}^+$  and  $^{22}\text{Na}^+$  versus  $^{22}\text{Ne}^+$  respectively. The final mass defects for the two isotopes of interest, after a  $-0.01 \text{ keV}$  correction for ionization energy differences, are then found to be  $\Delta M(^{22}\text{Mg}) = -399.73(67) \text{ keV}$  and  $\Delta M(^{22}\text{Na}) = -5181.12(29) \text{ keV}$ . They differ by  $-2.7 \text{ keV}$  and  $+1.3 \text{ keV}$  respectively from the latest tabulated values, in both cases well outside the tabulated error bars. In the first case, our result for the mass of  $^{22}\text{Mg}$  agrees with, but is much more precise than, the value extracted by a recent reevaluation of an older measurement,<sup>1</sup>  $-402(3) \text{ keV}$ , but is significantly higher than a recent measurement<sup>3</sup> of the  $^{21}\text{Na}(p,\gamma)^{22}\text{Mg}$  reaction, from which a mass defect of  $-403.2(13) \text{ keV}$  was inferred; the latter is, of course, also sensitive to the mass of  $^{21}\text{Na}$  and the excitation energy of the state populated in that reaction, both of which now

need to be remeasured. In the case of  $^{22}\text{Na}$ , the four previous measurements used to determine the tabulated mass date from 1972 or earlier and the three that disagree with our result were all derived from beta-decay end-point energies.

Our new mass results yield a  $Q_{\text{EC}}$  value of 4124.39(73) keV for the superallowed decay of  $^{22}\text{Mg}$  to the analog  $0^+$  state at 657.00(14)-keV excitation

energy in  $^{22}\text{Na}$ . This corresponds to an  $f$  value of 418.33(44). Taking this result, together with the branching ratio, 0.5315(12), and lifetime, 3.8755(12)s, and with the appropriate correction terms, we obtain a corrected  $Ft$  value of  $Ft = 3081(8)$  s, with the uncertainty now almost entirely due to the uncertainty of the branching ratio measurement. This value agrees with the 3072.2(8) s average  $Ft$  value for the nine well-known cases studied so far.

\*Argonne National Laboratory and University of Chicago, †Argonne National Laboratory and University of Manitoba, Winnipeg, Manitoba, ‡Argonne National Laboratory and University of Maryland, §McGill University, Montreal, Quebec, ¶Texas A&M University, ||University of Manitoba, Winnipeg, Manitoba, \*\*Queen's University, Kingston, Ontario.

<sup>1</sup>J. C. Hardy *et al.*, Phys. Rev. Lett. **91**, 082501 (2003).

<sup>2</sup>G. Audi *et al.*, Nucl. Phys. **A729**, 337 (2003).

<sup>3</sup>S. Bishop *et al.*, Phys. Rev. Lett. **90**, 162501 (2003).

### b.3. Q Value of the Superallowed Decay of $^{46}\text{V}$ and the Unitarity of the CKM Matrix

(G. Savard, J. A. Clark, A. A. Hecht, A. Levand, N. D. Scielzo, H. Sharma, K. S. Sharma, I. Tanihata, A. C. C. Villari, Y. Wang, F. Buchinger,\* J. E. Crawford,\* S. Gulick,\* J. K. P. Lee,\* and J.C. Hardy†)

Superallowed  $0^+ \rightarrow 0^+$  decays play a key role in a number of tests of the electroweak theory (see report on the  $^{22}\text{Mg}$   $Q$ -value measurement, section b.2.). In particular, they are used to obtain the most precise value of  $V_{ud}$  and test the CKM matrix unitarity. The data on the superallowed Fermi decays used to obtain the most precise value of  $V_{ud}$  come from over 100 different experiments. They contribute less than 20% of the total uncertainty on  $V_{ud}$ , the remainder coming from the small theoretical corrections that must be applied to the data. In particular, the corrections for nuclear structure effects, though not the largest contributors, have a significant impact on the uncertainty. One test of the latter corrections is to examine how precisely they convert the scatter in experimental  $f_t$  values to the CVC-predicted constancy of the  $Ft$  values. Improved precision for individual transitions sharpen that test. Of the nine most precisely known cases,  $^{46}\text{V}$  has the largest uncertainty associated with the  $Q$  value. We report here a  $Q$ -value measurement for the  $^{46}\text{V}$  decay, which yields a more precise  $Ft$  value for this superallowed transition. This new  $Q$  value disagrees with a previous measurement and uncovers a total of seven inconsistent  $Q$ -value measurements from the same reference that should be removed from the previously accepted data set. This leads to a significant change in the average of all  $Ft$  values and produces a change

in  $V_{ud}$ . It also impacts the derived limits on new physics.

The mass measurements were performed at the Canadian Penning Trap (CPT) mass spectrometer located "online" at the ATLAS accelerator. The  $^{46}\text{V}$  and  $^{46}\text{Ti}$  isotopes were created by a 3.3 MeV/u beam of  $^{36}\text{Ar}$  impinging on a 0.8 mg/cm<sup>2</sup> rotating target of natural carbon. Reaction products recoiling out of the target are separated from the primary beam and transported to a gas catcher system via a focusing magnetic quadrupole triplet, a velocity filter and an Enge magnetic spectrograph. The gas catcher system thermalizes these fast recoil ions in high-purity helium gas and extracts them as a low-energy doubly charged ion beam, suitable for injection into ion traps. The extracted ions are accumulated for 300 ms in a linear RF trap and transferred in a bunch to a gas-filled Penning trap where mass-selective cooling is applied. The ions are mass selected there with a resolving power of 1000 before being transported to the CPT spectrometer itself. The transport is performed in pulsed mode which allows further selection of the  $A/q = 23$  ions by time of flight. At the end of the time-of-flight system, the purified ions with  $A = 46$  and  $q = +2$  are captured in a second linear RF trap and further cooled by buffer-gas collisions before being transferred via a differential pumping section to the precision Penning trap where the mass measurements take place. The mass measurement takes place in a fashion similar to that described for the recent  $^{22}\text{Mg}$  measurement

(see section b.2.) except that the doubly charged ions allow us to reach higher resolution for a given

interaction time. Typical frequency scans obtained for the isotopes  $^{46}\text{V}^{2+}$  and  $^{46}\text{Ti}^{2+}$  are shown in Fig. I-9.

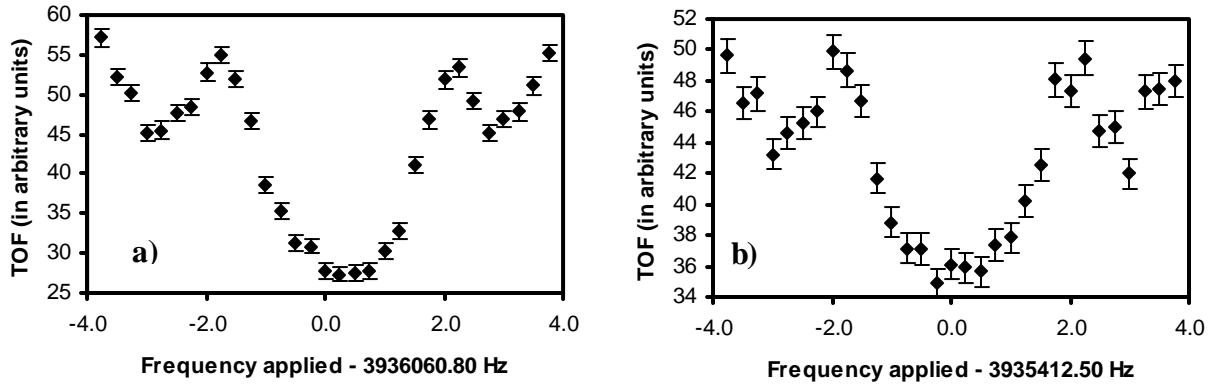


Fig. I-9. Time-of-flight spectra obtained for  $^{46}\text{Ti}^{2+}$  (a) and  $^{46}\text{V}^{2+}$  (b) using a quadrupole excitation of 500 ms duration. The mass resolution is  $\sim 5 \times 10^{-7}$ .

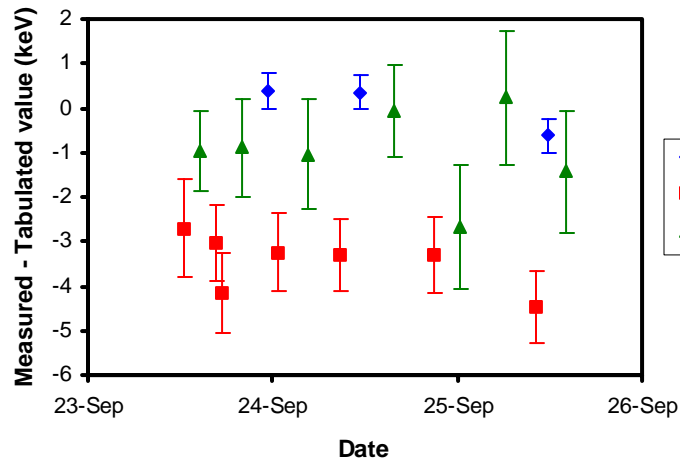


Fig. I-10. Measured mass values (plotted as deviations from the tabulated mass values [10]) for the isotopes of interest versus time during the experiment.

The experiment interleaved measurements of the mass of  $^{46}\text{V}^{2+}$  and  $^{46}\text{Ti}^{2+}$  with calibrations of the magnetic field via measurements of  $^{22}\text{Ne}^+$  (see Fig. I-10). A small magnetic-field drift (about  $8 \times 10^{-10}$  per hour) was observed during the experiment. This shift is negligible at the level of accuracy required since calibration and measurements on radioactive species were interleaved; nevertheless all measure-

ments were corrected for it. The results of the different measurements are then averaged with the proper statistical weights to yield the final values for the cyclotron frequencies and statistical uncertainties. The resulting cyclotron frequency ratios are:  $\nu(^{46}\text{V}^{2+})/\nu(^{22}\text{Ne}^{1+}) = 0.956974161(12)$ ,  $\nu(^{46}\text{Ti}^{2+})/\nu(^{22}\text{Ne}^{1+}) = 0.957131846(10)$  and  $\nu(^{46}\text{V}^{2+})/\nu(^{46}\text{Ti}^{2+}) = 0.999835252(9)$ .

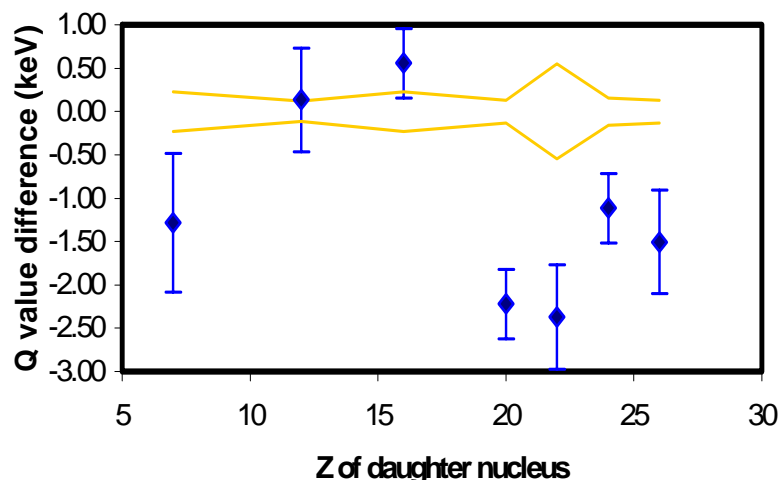


Fig. I-11. Difference between the  $Q$  values measured by Vonach et al.,<sup>3</sup> (blue diamonds) and the values obtained from all other data. The lines indicate the uncertainty on the relevant  $Q$  values from the other existing data.

Measurements on the  $^{46}\text{V}$ ,  $^{46}\text{Ti}$  and  $^{22}\text{Ne}$  isotopes were performed with an average of 0.34 ions, 1.02 ions and 1.18 ions detected per cycle respectively. Shifts in cyclotron frequency due to ion-ion interactions for different number of ions in the trap were measured with  $^{22}\text{Ne}$  isotopes to be  $-1.7(2.7)$  ppb per detected ion, under the conditions used during the experiment. Corrections to the three frequency ratios given above of  $1.4(2.3) \times 10^{-9}$ ,  $0.3(4) \times 10^{-9}$  and  $1.2(1.8) \times 10^{-9}$  respectively were applied to account for this effect. The spatial extent probed by the ions in the trap is determined by the ion preparation and the conditions of injection. Optimization of the injection conditions to minimize possible systematic errors will be performed following a procedure outlined in section h.3. For measurements of isotopes with different  $A/q$  ratios this procedure yields an accuracy better than  $10^{-8}$ ; for species with the same  $A/q$  ratio the conditions are identical and no uncertainty is introduced. We use the demonstrated 1 part per  $10^8$  accuracy as a conservative value for our systematic uncertainty for the new mass values obtained below from ratios of isotopes with different mass number. The masses of the two  $A = 46$  isotopes can be obtained from the frequency ratios to the well-known mass of  $^{22}\text{Ne}$ , after correction for the missing electron mass (or two electron masses) and the electronic binding energies. This yields mass values of  $m(^{46}\text{V}) = 45.96019909(69)$  amu and  $m(^{46}\text{Ti}) = 45.95262748(62)$  amu. Our result for  $^{46}\text{Ti}$  differs substantially from the value in the 2003 mass tables. It should however be noted that this latter value depends on a 30-year-old unpublished (p, $\gamma$ ) measurement.<sup>1</sup>

The  $Q$  value for the decay can be obtained more precisely from the ratio of the cyclotron frequencies for  $^{46}\text{V}$  and  $^{46}\text{Ti}$  directly since most systematic effects (with the exception of the ion number dependency which is corrected for) cancel out for such a close doublet of masses. The measured ratio yields, after corrections, a  $Q$  value for the superallowed decay of  $7052.90(40)$  keV, which differs by 2.19 keV from the value determined in the latest compilation<sup>2</sup> (from the average of two mutually-inconsistent results:  $7053.3(1.8)$  and  $7050.41(60)$  keV). The present measurement agrees with the first of those but is in strong disagreement with the second one,<sup>3</sup> which claims smaller error bars. This second result originated from ( $^3\text{He},t$ ) reaction measurements in a Q3D spectrometer calibrated with a beam whose energy was measured with a time-of-flight system. These measurements actually included results<sup>3</sup> on a total of seven high-precision  $Q$  values of superallowed emitters and we therefore undertook a reassessment of all seven. In Fig. I-11 we compare the  $Q$  values obtained in Ref. 3 to those we obtain using all data from a recent compilation<sup>2</sup>, including our new measurement, but excluding Ref. 3. The deviations average more than  $2\sigma$  and peaks at  $5\sigma$ . The probability that the deviations of the results from Ref. 3 are due to statistical fluctuations is below 0.0000001%. Since the energy calibration used in Ref. 3 cannot be traced back and the deviations appear to not only be large but also predominantly in one direction, we have opted to remove these measurements from the high precision data set. The resulting precision data set (Table I-1) yields the  $Ft$  value plot shown in Fig. I-12. The agreement amongst the various emitters is still remarkable. The average  $Ft$  value for the most precise 12 cases is now shifted to  $3073.66(75)$ , one standard deviation above the latest

evaluation, with a reduced  $\chi^2$  of 1.12. The increase in the reduced  $\chi^2$  is due mainly to the new  $Ft$  value for  $^{46}\text{V}$ ,  $Ft(^{46}\text{V}) = 3079.9(23)\text{s}$ , with the neighboring decays  $^{42}\text{Sc}$  and  $^{34}\text{Cl}$  also contributing slightly. This might be a first clear indication of deviations from the calculated isotope-to-isotope variation in nuclear-structure-dependent corrections that we ultimately aim to test. This poorer reduced  $\chi^2$  is also reflected in a slightly weaker scalar current limit than that obtained in Ref. 2, the Fierz interference term now being  $b_F = 0.0024(28)$ . For the  $^{46}\text{V}$  decay, the  $Q$  value and lifetime measurements now have roughly similar contributions to the total experimental error, both being smaller than the uncertainty in the

nuclear-structure-dependent corrections. The  $Ft$  values for both  $^{46}\text{V}$  and  $^{42}\text{Sc}$  are significantly above the average and in both cases the values were raised with respect to the other emitters by the calculated corrections. An independent calculation of these nuclear structure dependent corrections yields a slightly higher average  $Ft$  value but the same general variations from emitter to emitter. A reevaluation of the variations in these calculations may be warranted but at present we follow Ref. 2 and use the mean value for these corrections for the nine most precise cases (for which both calculations are available), assigning a systematic uncertainty equal to half the mean difference. This yields a new average  $Ft = 3074.4(12)\text{s}$ .

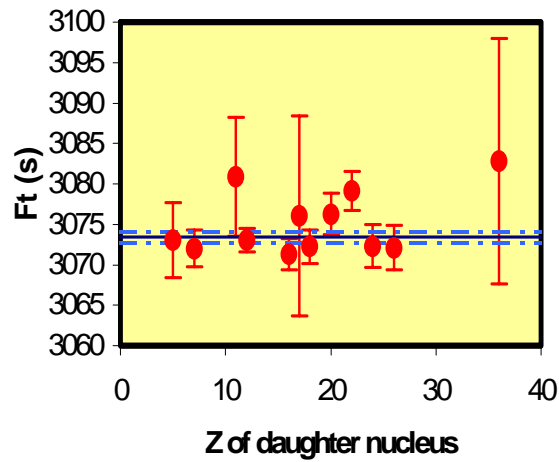


Fig. I-12.  $Ft$  values for the most precisely known superallowed beta emitters with the modified data set.

Table I-1. New values for the  $ft$  values and corrected  $Ft$  values for the 12 most precisely known cases obtained with the modified data set.

Emitter	$ft$ -value	$Ft$ -value
$^{10}\text{C}$	3039.5(47)	3073.0(49)
$^{14}\text{O}$	3043.3(19)	3072.0(26)
$^{22}\text{Mg}$	3052.4(72)	3080.9(74)
$^{26\text{m}}\text{Al}$	3036.8(11)	3073.0(15)
$^{34}\text{Cl}$	3050.0(12)	3071.2(19)
$^{34}\text{Ar}$	3060(12)	3076.6(123)
$^{38\text{m}}\text{K}$	3051.1(10)	3072.2(21)
$^{42}\text{Sc}$	3046.8(12)	3076.4(24)
$^{46}\text{V}$	3050.7(12)	3079.9(23)
$^{50}\text{Mn}$	3045.8(16)	3072.4(27)
$^{54}\text{Co}$	3048.4(11)	3072.2(28)
$^{74}\text{Rb}$	3084.3(80)	3083.3(154)

With the new average  $Ft$  value and the transition independent radiative corrections one obtains a new value for the weak vector coupling constant of  $G_V/(\hbar c)^3 = 1.1356(5) \times 10^{-5} \text{ GeV}^{-2}$ . Combining this

value with the Fermi coupling constant one obtains a new value of  $V_{ud} = 0.9736(4)$ . This value is lower than that obtained in the latest evaluation of superallowed decay data but is still within the previously quoted uncertainty.

Before proceeding to the unitarity sum of the top row of the CKM matrix, we must first decide on an appropriate value for  $V_{us}$ . Recent results from BNL-E865,<sup>4</sup> KTeV,<sup>5</sup> NA48,<sup>6</sup> and KLOE<sup>7</sup> yield values for  $|V_{us}f_+(0)|$  consistently higher than the values quoted by the Particle Data Group.<sup>8</sup> Various calculations are available for  $f_+(0)$  but following most authors we use the value from Czarnecki *et al.*<sup>9</sup> which yields, with the weighted average of the above experimental results,  $V_{us} = 0.2248(19)$ . Using this value together with our new value for  $V_{ud}$  and the PDG<sup>8</sup> value for  $V_{ub}$ , we obtain

$$V_{ud}^2 + V_{us}^2 + V_{ub}^2 = 0.9985 \pm 0.0012;$$

with equal contributions to the uncertainty coming from  $V_{ud}$  and  $V_{us}$ . For both elements, the uncertainty is dominated by uncertainty in theoretical calculations ( $f_+(0)$  for  $V_{us}$  and  $\Delta V_R$  for  $V_{ud}$ ).

In conclusion, a high-precision determination of the  $Q$  value of the superallowed decay of  $^{46}\text{V}$  has resolved a discrepancy in that value and uncovered a set of seven measured  $Q$  values that systematically disagree with this and other precise results from the

data set used for the most precise determination of  $V_{ud}$ . A new evaluation has been performed with a revised data set that includes the present measurement and excludes the seven faulty values. It yields a lower value for  $V_{ud}$  that, when combined with the recently improved value for  $V_{us}$ , almost satisfies CKM unitarity in the top-row test ( $V_{us}$  has moved towards unitarity while  $V_{ud}$  is being moved slightly away by our measurement). The precision of that test is now dominated by theoretical uncertainties in the determination of both  $V_{ud}$  and  $V_{us}$ . The CVC test connected to the constancy of the  $Ft$  values measured in superallowed decays has been worsened slightly by the changes to the data set, as has been the limit on scalar currents.

This measurement marked the first online precision mass measurement on a doubly-charged short-lived isotope in a Penning trap and the gain in resolution yielded a better than  $10^{-8}$  accuracy in the mass ratio, the highest achieved online so far by any system. An extension of these precision measurement techniques to the other superallowed emitters is necessary to shed more light on the current situation and this is ongoing at the CPT at ATLAS.

\*McGill University, Montreal, Quebec, †Texas A&M University.

<sup>1</sup>G. Guillaume (1971), thesis, Universite de Strasbourg.

<sup>2</sup>J. C. Hardy and I. S. Towner, Phys. Rev. C **71**, 055501 (2005).

<sup>3</sup>H. Vonach *et al.*, Nucl. Phys. **A278**, 189 (1977).

<sup>4</sup>A. Sher *et al.*, Phys. Rev. Lett. **91**, 261802 (2003).

<sup>5</sup>T. Alexopoulos *et al.*, Phys. Rev. Lett. **93**, 181802 (2004).

<sup>6</sup>A. Lai *et al.*, Physics Letters **B602**, 41 (2004).

<sup>7</sup>P. Franzini (2004), hep-ex/0408150.

<sup>8</sup>S. Eidelman *et al.*, Phys. Lett. **B592**, 1 (2004).

<sup>9</sup>A. Czarnecki *et al.*, Phys. Rev. D **70**, 093006 (2004).

#### **b.4. Precise Mass Measurement of Light Fission Fragments from $^{252}\text{Cf}$ Source** (Y. Wang, H. Sharma, G. Savard, A. Levand, K. S. Sharma, J. Wang, and Z. Zhou)

The injection system of the CPT mass spectrometer is versatile enough to allow radioactive ions produced using various techniques to be injected into the ion trap system effectively. After successful measurements on heavy neutron-rich fission fragments, we have started measurements on the light fragments produced by  $^{252}\text{Cf}$  fission. Nine neutron-rich isotopes  $^{106,107}\text{Mo}$ ,  $^{107,108}\text{Tc}$ ,  $^{108-111}\text{Ru}$ , and  $^{111}\text{Rh}$  from the light  $^{252}\text{Cf}$  fission fragment peak have been measured with the CPT mass spectrometer to a few tens of keV/c<sup>2</sup> precision and compared with the most recent atomic mass evaluation (AME 2003). In these

measurements, the gas catcher stops the light fission fragments produced by the  $^{252}\text{Cf}$  fission source located just outside the gas cell and guides them to the exit nozzle of the cell by a combination of the 150 Torr pure Helium gas flow, radio frequency (RF) and DC electric fields. The light fission fragments with mass around 110 amu differ from the heavy fragments studied previously in that they are stopped much less efficiently in the gas and are extracted from the gas catcher system mostly as singly-charged particles. After cooling and bunching in the RFQ cooler, the ions are ejected into a mass selective ion trap which purifies them with a mass resolution of about 800

at mass 100 using a recentering RF amplitude of  $0.25V_{pp}$ . About 400 ms duration time is required in this trap to separate the desired isotopes from the contaminant molecules. About 95% of the contaminant ions can be removed in the mass selective trap. The ions of interest are further selected by time-of-flight technique using a gated  $0.1 \mu\text{s}$  deflection pulse that only transmits ion of a single  $A/q$  to a gas-filled RFQ linear trap where further cooling takes place before the ions are finally delivered to the Penning trap where the precise mass measurement takes place. A 500 ms excitation time for cyclotron frequency  $\omega_c$  was employed for all of the light fission fragments measurements and yields a resolving power of about 450000 and a  $10^{-7}$  precision. The CPT measurements of  $^{107}\text{Mo}$ ,  $^{107,108}\text{Tc}$ , and  $^{108,109,111}\text{Ru}$  have better precision than the AME2003 values. Only  $^{108}\text{Tc}$ ,  $^{108,110}\text{Ru}$ , and  $^{111}\text{Rh}$  are found to agree with the mass table, within errors, a situation which is not unexpected in a

neutron rich region that has been difficult to access previously. In general, the measured masses are larger than predicted from systematic trends, i.e., the nuclei are less bound than expected (Fig. I-13).

These light fission fragment measurements have benefited from a number of improvements to the CPT system that were implemented in 2004. A  $450 \mu\text{Ci}$   $^{252}\text{Cf}$  fission source, which is ten times stronger than the previously used source, was installed in front of the  $1.9 \text{ mg/cm}^2$  thickness Havar window of the gas catcher. The activities counted on the silicon detectors increased by about a factor of ten (but so did the observed contaminants). A new cleaning system was installed to provide all the  $\omega_+$  cleaning frequencies together in a cosine envelope with 100 ms duration time. The new cleaning system enables us to measure shorter-lived isotopes by saving several hundreds millisecond in the sample preparation in the final Penning trap.

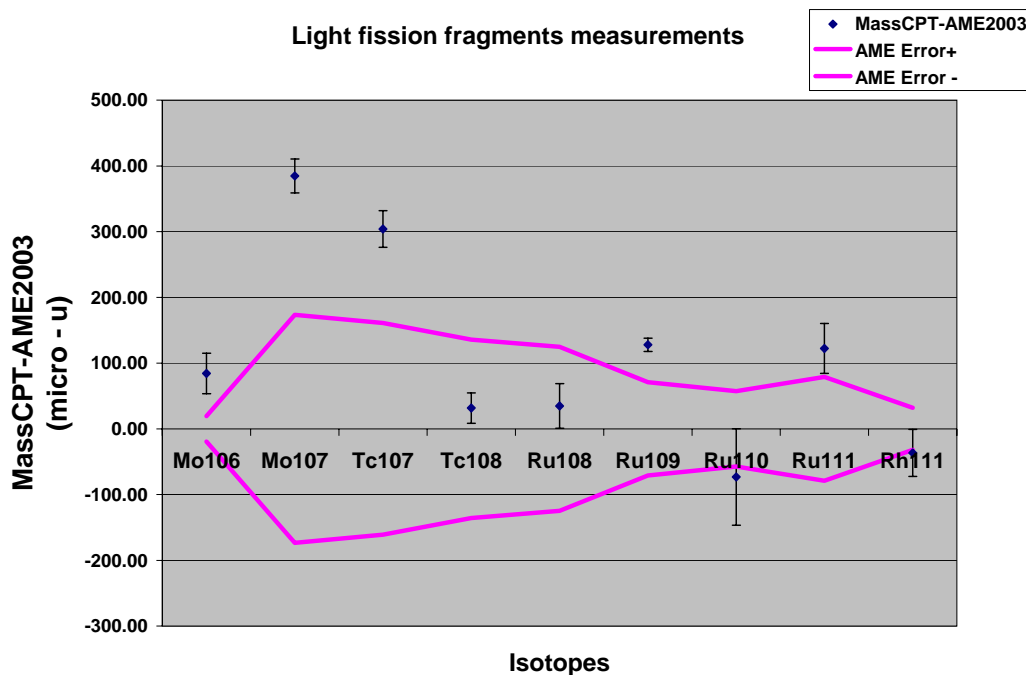


Fig. I-13. Mass comparisons between CPT measured values and the AME2003 values ( $1 \mu\text{u} \sim 0.93 \text{ keV}$ ).

### b.5. The RFQ Decay Trap Component of the Advanced Penning Trap System

(N. D. Scielzo, G. Savard, J. A. Clark, S. Gulick, A. A. Hecht, A. Levand, H. Sharma, K. S. Sharma, I. Tanihata, A. Villari, J. Wang, Y. Wang, Z. Zhou, and B. J. Zabransky)

The installation of a RFQ decay trap as part of the Advanced Penning Trap (APT) system is nearing completion in preparation for a first loading with

radioactive ions for precision  $\beta$ -decay measurements. Trapped radioactive ions are a nearly ideal source of activity for measurements of the  $\beta$ - $\nu$  correlation

coefficient,  $a$ , since scattering of the recoiling daughter nuclei (with energy  $\sim 100$  eV) is essentially eliminated and the neutrino momentum can be inferred from the recoil of the nucleus. Although the tightest constraints on interactions beyond the dominant V - A terms come from measurements of  $a$ , contributions from scalar and tensor interactions as large as 10% of the vector and axial-vector terms are not excluded.<sup>1,2</sup> By detecting  $\beta$ - $\gamma$  coincidences in the superallowed  $0^+$  to  $0^+$  Fermi decay of  $^{14}\text{O}$ , the momentum of the recoil nucleus can be inferred from the Doppler shifts of the deexciting 2.313 MeV  $\gamma$ -rays.

The transfer of ions from the isobar separator to the decay trap was simulated using SIMION 7.0 and the

required ion optics elements were constructed. We anticipate nearly 100% efficiency in transfer of ions from the isobar separator trap to the RFQ decay trap. The vacuum chamber to hold the newly constructed RFQ decay trap was built and placed in position in the beamline. Figure I-14 shows the open vacuum chamber with the RFQ trap inside and one HPGe detector held in place. Within the vacuum system, the cabling for the Si detector telescopes, LN<sub>2</sub> and He gas feedthroughs, and thermocouple connections were constructed with UHV-compatible parts to ensure purity of the He buffer gas used to cool the trapped ions. Any impurities in the buffer gas could lead to ion loss from the trap. Decays from untrapped ions would be difficult to distinguish from those of trapped ions and lead to a background that causes a systematic shift in measurements of the  $\beta$ - $\nu$  correlation.

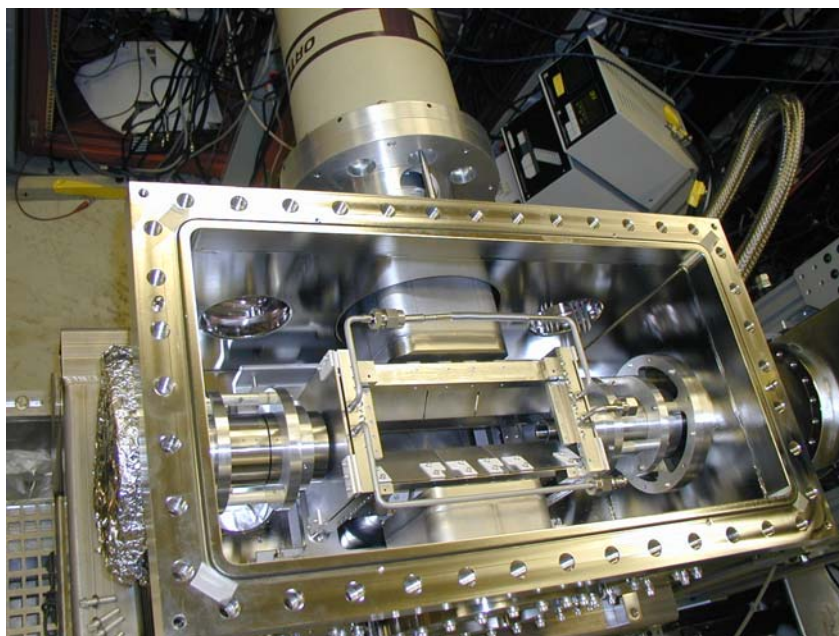


*Fig. I-14. Photo of the RFQ vacuum chamber opened to show the RFQ trap. Several pieces of the trap and the Si detectors have been removed to provide a view of the traps interior and electrode plates. One HPGe detector in a re-entrant port is visible. The re-entrant port on the bottom of the chamber is not visible and the fourth one is attached to the chamber lid.*

The data acquisition to be used to record  $\beta$ - $\gamma$  coincidences was tested "offline" with the Si detectors using radioactive sources. RF pick-up (from the trapping fields) on the Si detector telescopes was eliminated by placing a grounded shield around the detectors. The re-entrant ports that enable the HPGe detectors to be brought within 4" of the trapped ion cloud were constructed. The ends of these ports have a 1/16" stainless steel vacuum window to minimize the attenuation of  $\gamma$ -rays. The detector supports attach to the re-entrant port flanges

and allow for precision positioning of the HPGe detectors.

GEANT4 simulations of  $\beta$ -decay of  $^{14}\text{O}$  within the trap show that the largest systematic effect in the current geometry is likely to be from positron scattering. The required correction can be reduced to only  $\sim 1\%$  by replacing the stainless steel electrodes with beryllium ones and placing beryllium plates on the grounded RF shields. The simulations showed that other potential systematic effects, such as the achievable Si and HPGe

detector positioning (<1 mm) and energy calibration leads to systematic uncertainties of only  $\sim 0.2\%$  in  $a$ .

The statistical precision required of a competitive measurement of the  $\beta$ - $\nu$  correlation coefficient,  $a$ , requires a low-energy  $^{14}\text{O}^{1+}$  beam with intensities of  $\sim 10^5$  ions/sec. Therefore, the  $^{14}\text{O}$  produced must be transported through the system with maximum efficiency. An initial production run using the  $p(^{14}\text{N}, ^{14}\text{O})n$  reaction demonstrated the ability of the system to transport  $^{14}\text{O}^{1+}$  from the gas target to the isobar separator trap. However, the transportation efficiency was a factor 100 less than anticipated. Although the optimal gas catcher settings have been determined for ions of mass  $A \sim 100$ , the best settings for mass 14 amu are still being determined. New tunable RF feeding circuits were installed on the

cooler of the gas catcher to improve the transmission for light ions. The efficiency for extracting  $^{14}\text{O}^{1+}$  from the cone of the gas catcher was also improved as the RF frequency applied to the cone was increased from the normal value for heavy ions of roughly 750 kHz up to about 1.6 MHz. The frequency could however not be increased further due to capacitors within the vacuum system, and as a result the gas catcher had to be operated at a lower than optimal electric field setting. Installing new capacitors will enable us to reach higher frequencies and reach an efficiency of the gas catcher for these light masses similar to what is reached for heavier ions and obtain the required  $10^5$  cooled  $^{14}\text{O}$  ions per second.

It is anticipated that the RFQ trap will be loaded in Fall 2005 for the first  $\beta$ - $\gamma$  correlation measurements.

<sup>1</sup>A. I. Boothroyd, J. Markey, and P. Vogel, Phys. Rev. C **29**, 603 (1984).

<sup>2</sup>E. G. Adelberger *et al.*, Phys. Rev. Lett. **83**, 1299 (1999).

